Adiabatic quantum imaginary time evolution

Kasra Hejazi [ORCID],[1] Mario Motta,[2] and Garnet Kin-Lic Chan[1]

[1]*Division of Chemistry and Chemical Engineering, California Institute of Technology, Pasadena, California 91125, USA*
[2]*IBM Quantum, Almaden Research Center, San Jose, California 95120, USA*

We introduce an adiabatic state preparation protocol which implements quantum imaginary time evolution under the Hamiltonian of the system. Unlike the original quantum imaginary time evolution algorithm, adiabatic quantum imaginary time evolution does not require quantum state tomography during its runtime and, unlike standard adiabatic state preparation, the final Hamiltonian is not the system Hamiltonian. Instead, the algorithm obtains the adiabatic Hamiltonian by integrating a classical differential equation that ensures that one follows the imaginary time evolution state trajectory. We introduce some heuristics that allow this protocol to be implemented on quantum architectures with limited resources. We explore the performance of this algorithm via classical simulations in a one-dimensional spin model and highlight essential features that determine its cost, performance, and implementability for longer times, and compare to the original quantum imaginary time evolution for ground-state preparation. More generally, our algorithm expands the range of states accessible to adiabatic state preparation methods beyond those that are expressed as ground states of simple explicit Hamiltonians.

I. INTRODUCTION

A central step in the quantum simulation of physical systems is to prepare a relevant initial state. Taking ground-state simulation as an example, we typically wish to prepare a state with sufficient overlap with the desired ground-state $|\Psi_0\rangle$ of a Hamiltonian H. In the context of near-term quantum algorithms [1], which minimize both qubits/ancillae and gate resources, many protocols for such ground-state preparation have been proposed. Examples include variational ansatz preparation [2–7], adiabatic state preparation (ASP) [8–10], and variational [11] and quantum imaginary time evolution (QITE) [12–18], the latter being the subject of this work.

Because ground-state preparation is in general formally hard, all these methods rely on some assumptions. For example, ASP starts from an initial Hamiltonian $H(0)$, whose ground state is simple to prepare, and defines an adiabatic path $H(s)$, $0 \leqslant s \leqslant 1$, with $H(1) \equiv H$, the desired Hamiltonian [19]. To prepare the ground state to sufficient accuracy, $H(s)$ must change slowly; an estimate of the adiabatic runtime is [8,20] $T \sim \max_{s,j} \frac{|\langle \Psi_j(s)|dH/ds|\Psi_0(s)\rangle|}{\Delta^2}$, where $|\Psi_0(s)\rangle$, $|\Psi_j(s)\rangle$, with $j \geqslant 1$, denote the instantaneous ground and excited states of $H(s)$ and $\Delta(s)$ is the energy gap between the ground state and the first excited state. For ASP to be efficient, $H(s)$ must be chosen such that $\min_s \Delta(s)$ is not too small, e.g., at worst $1/\mathrm{poly}(L)$ in system size L, for a polynomial cost algorithm.

The QITE algorithm [12], on the other hand, applies $e^{-H\tau}$ ($\tau > 0$) to boost the overlap of a candidate state with the ground state of H; for this work, we consider Hamiltonians that are sums of local terms $H = \sum_\alpha h_\alpha$, where h_α is geometrically local (i.e., each term h_α acts on a constant number of adjacent qubits regardless of system size). Reference [12] introduced a near-term quantum algorithm to obtain the states

$$|\Psi(\tau)\rangle = e^{-H\tau}|\Psi(0)\rangle \,/\, \||e^{-H\tau}|\Psi(0)\rangle\|, \tag{1}$$

without employing any ancillae or postselection. The method is efficient if $|\Psi(\tau)\rangle$ has finite correlation volume C for all earlier imaginary times, in which case $|\Psi(\tau)\rangle$ can be prepared by implementing a series of local unitaries acting on $O(C)$ qubits on the candidate state. By using this technique which reproduces the imaginary time trajectory, one can also use QITE as a subroutine in other ground-state algorithms, as well as to prepare nonground states and thermal (Gibbs) states, for example, by reintroducing ancillae [17], or by sampling [12].

However, to find the unitaries in QITE one needs to perform tomography [12] of the reduced density matrices of $|\Psi(\tau)\rangle$ over regions of volume C. Although the measurement and processing cost is polynomial in system size, it can still be prohibitive for large C. Despite various improvements in the QITE idea in terms of the algorithm and implementation, this remains a practical drawback [13]. [We briefly note also some other near-term imaginary time evolution algorithms, such as the variational ansatz-based quantum imaginary time evolution, introduced in Ref. [11], which reproduces the imaginary time evolution trajectory in the limit of an infinitely flexible variational ansatz, as well as the probabilistic imaginary time evolution algorithm (PITE) [21], whose probability of success decreases exponentially with evolution time.]

Here, we introduce an alternative near-term, ancilla-free, quantum method that generates the imaginary time evolution of a quantum state without any tomography. It thus eliminates one of the resource bottlenecks of the original QITE. The idea is to consider the imaginary time trajectory $\Psi(\tau)$ as generated by an adiabatic process under a particular Hamiltonian $\tilde{H}(\tau)$. This adiabatic Hamiltonian is approximated by the solution of an auxiliary dynamical equation that can be solved entirely classically, i.e., without any feedback from the quantum simulation. Although propagation under $\tilde{H}$ reproduces imaginary time evolution when performed adiabatically [i.e., one stays in the ground state of $\tilde{H}(\tau)$], this is different to the usual ASP, because $\tilde{H}$ does not approach H at the end of the path, even though it shares the same final ground state. We thus refer to this algorithm as adiabatic quantum imaginary time evolution or A-QITE.

Like QITE, the application of A-QITE for sufficiently long imaginary time formally prepares the ground state. But also like QITE, the imaginary time trajectory generated by A-QITE has other applications. The ability to reproduce nonunitary evolution enables applications to Lindblad simulation [17], while for finite imaginary time, it can naturally be applied to prepare thermal states (either in a purified formulation [17] or via sampling [12,13]) or be used in a subspace expansion method for excited states [12]. Generally speaking, the A-QITE algorithm turns the preparation of any state that can be reached by the differential evolution of an initially known ground state into an adiabatic state preparation process. In this work, however, we primarily focus on the generation of the imaginary time trajectory itself and its long-time limit relevant to physical ground-state preparation.

We examine the feasibility and performance of A-QITE for the illustrative case of the Ising-like Heisenberg XXZ model in a transverse field. There we study the behavior of the instantaneous gap and norm of $\tilde{H}$ as a function of imaginary time (as these determine the cost of integrating the classical equation to determine $\tilde{H}$ as well to implement the adiabatic quantum simulation under $\tilde{H}$). $\tilde{H}(\tau)$ becomes increasingly nonlocal with time and we introduce a geometric locality heuristic to truncate terms in $\tilde{H}$, which we compare to the original inexact QITE procedure. We finish with some observations on the cost and practical implementation of the algorithm.

II. FORMALISM

A. General theory

Consider a lattice system described by a Hamiltonian H. We desire an adiabatic Hamiltonian $\tilde{H}(\tau)$ whose ground state at every τ is given by Eq. (1). Consider an infinitesimally imaginary time evolved state from τ to $\tau + d\tau$:

$$|\Psi(\tau + d\tau)\rangle = |\Psi(\tau)\rangle - d\tau \, QH|\Psi(\tau)\rangle + O(d\tau^2), \quad (2)$$

where $Q = 1 - |\Psi(\tau)\rangle\langle\Psi(\tau)|$ projects out the ground subspace. Now, suppose $|\Psi(\tau)\rangle$ is the ground state of $\tilde{H}(\tau)$; one should determine $\tilde{H}(\tau + d\tau) = \tilde{H}(\tau) + \delta\tilde{H}$ such that $|\Psi(\tau + d\tau)\rangle$ is its ground state: perturbation theory determines the ground state of $\tilde{H}(\tau + d\tau)$ as $|\Psi(\tau)\rangle + [\tilde{E}_0 - \tilde{H}(\tau)]^{-1}Q \, \delta\tilde{H}|\Psi(\tau)\rangle$, where $\tilde{E}_0$ is the smallest eigenvalue of $\tilde{H}$. We will be working with evolution schemes for $\tilde{H}$ that start

with and maintain $\tilde{E}_0 = 0$ (more on this below). Thus using (2) we should have

$$\delta\tilde{H}|\Psi(\tau)\rangle = d\tau \, \tilde{H}H|\Psi(\tau)\rangle + O(d\tau^2), \quad (3)$$

where we have used $\tilde{H}Q = Q\tilde{H} = \tilde{H}$.

Equation (3) is the main equation the adiabatic Hamiltonian $\tilde{H}$ should satisfy. However, it does not uniquely determine $\delta\tilde{H}$ and so there are many generating equations for $\tilde{H}$. A simple choice is

$$\frac{d\tilde{H}}{d\tau} = \tilde{H}H + H\tilde{H}, \quad (4)$$

where we have used $\tilde{H}|\Psi(\tau)\rangle = 0$ [see above Eq. (5) for justification] and added the term $H\tilde{H}$ to make the right-hand side Hermitian. This has the formal solution $\tilde{H}(\tau) = e^{H\tau}\tilde{H}(0)e^{H\tau}$ [where $\tilde{H}(0)$ is chosen so that $\Psi(0)$ is its ground state with zero eigenvalue]. The above scheme can, in principle, be implemented as a hybrid quantum-classical algorithm, where $\tilde{H}$ is first determined by the classical integration of Eq. (4) and then used to implement adiabatic state evolution quantumly. [In other words, we carry out Hamiltonian dynamics with $\tilde{H}(\tau)$ along the adiabatic path $\tau = 0 \ldots \beta$, which, if performed slowly (see below), will guarantee that one remains in the ground state of $\tilde{H}(\tau)$; the dynamics can be translated into a circuit using standard Hamiltonian simulation techniques [2]]. As is clear, this procedure does not involve any feedback from the quantum simulation and thus does not involve tomography, unlike the original QITE.

In addition, the above procedure can be used to generate an adiabatic Hamiltonian $\tilde{H}(\tau)$ to prepare states beyond $e^{-\beta H}|\Psi(0)\rangle$, generalizing to the class of states $\mathcal{T} e^{-\int_0^\beta d\tau' L(\tau')}|\Psi(0)\rangle$, where $L(\tau')$ is an arbitrary operator that need not even be Hermitian. This can be seen by considering each time step of propagating $L(\tau)$ separately and decomposing L into a sum of Hermitian and anti-Hermitian parts $L_H + L_{AH}$. The time evolution reads $d\tilde{H}/d\tau = \{\tilde{H}(\tau), L_H(\tau)\} + [\tilde{H}(\tau), L_{AH}(\tau)]$. Thus a wide class of states, beyond ground states or physical imaginary time-evolved states, become accessible through an adiabatic state evolution (assuming a nonvanishing gap).

However, this naive scheme has some potential problems. One set is analogous to that encountered in the original quantum imaginary time evolution scheme, namely, the time evolution of $\tilde{H}$ renders it nonlocal (both geometrically and in terms of the lengths of the Pauli strings in $\tilde{H}$) and increasingly complicated. For example, even if $H = \sum_\alpha h_\alpha$ and $\tilde{H} = \sum_\beta \tilde{h}_\beta$ are geometrically local, the time derivative introduces geometrically nonlocal terms like $h_\alpha \tilde{h}_\beta$ and the number of such terms grows exponentially with time (the exponent in the rate of increase of Pauli strings with significant coefficients depends on the details of h_α) up until the maximum number of 4^L, where L is the size of the lattice. This renders both the classical determination of $\tilde{H}(\tau)$ and the quantum implementation of state evolution under $\tilde{H}(\tau)$ inefficient for large τ.

There is also a second set of problems arising from the norm of $\tilde{H}$ and its spectrum. We use the symbol $|\tilde{\phi}_i(\tau)\rangle$ to denote the instantaneous eigenstate of $\tilde{H}(\tau)$ with eigenvalue $\tilde{E}_i(\tau)$ [if $\tilde{H}$ implements the imaginary time evolution perfectly, then $|\tilde{\phi}_0(\tau)\rangle = |\Psi(\tau)\rangle$]. Taking expectation values

of Eq. (4) with $|\tilde{\phi}_i\rangle$, the eigenvalues of $\tilde{H}$ evolve as $\frac{d\tilde{E}_i}{d\tau} = 2\tilde{E}_i\langle\tilde{\phi}_i|H|\tilde{\phi}_i\rangle$. If $\tilde{H}$ is initialized with zero ground-state energy, the evolution will keep it vanishing. However, the other eigenvalues evolve as

$$\tilde{E}_i(\tau) = \exp\left[2\int_0^\tau d\tau' \langle\tilde{\phi}_i(\tau')|H|\tilde{\phi}_i(\tau')\rangle\right]\tilde{E}_i(\tau=0). \quad (5)$$

To see the potential problems with this, consider the example where H has a finite spectrum with all eigenvalues above (or below) 0. In that case, we clearly see that the eigenvalues $\tilde{E}_i$, $i > 0$ are always growing (shrinking) with time, potentially exponentially fast. Thus there is the possibility for numerical issues at long times in determining $\tilde{H}$ and implementing evolution under it, as we now discuss.

The integration of the classical differential equation for $\tilde{H}$ and the corresponding time evolution under $\tilde{H}$ will carry some finite numerical error which depends on $||\tilde{H}||$. This means that rather than obtaining the exact $\tilde{H}(\tau)$, we obtain $\tilde{H}(\tau) + V$; if one uses, e.g., a finite-order Runge-Kutta method, then $||V|| \propto ||\tilde{H}||$. Depending on the dynamics of the eigenvalues, this may introduce a large deviation from the instantaneous ground state, for example, if $|\langle\tilde{\phi}_0|V|\tilde{\phi}_i\rangle/\tilde{\Delta}_i| \gg 1$ (where $\tilde{\Delta}_i$ is the instantaneous gap to the ith state of $\tilde{H}$). Similarly, the quantum adiabatic evolution time depends on $||\tilde{H}(\tau)||$: since $\max_s ||d\tilde{H}/ds/\tilde{\Delta}(s)^2|| \propto \beta||H|| \max_\tau ||\tilde{H}(\tau)/\tilde{\Delta}(\tau)^2||$, the total adiabatic evolution time $T \propto \beta||H|| \max_\tau ||\tilde{H}(\tau)/\tilde{\Delta}(\tau)^2||$, which can diverge if the numerator is exponentially growing or the denominator is exponentially decreasing. As a result, we will be focused on studying the behavior of $||\tilde{H}(\tau)||$ and $\tilde{\Delta}(\tau)$ numerically below (especially their behavior with total imaginary time and length). Finally, the implementation of Hamiltonian simulation under $\tilde{H}(\tau)$ also introduces errors that grow polynomially with $||\tilde{H}||$ (see, e.g., Corollary 2 of [22]).

The appearance of such problems might be considered natural given that reproducing the imaginary time trajectory as $\beta \to \infty$ is equivalent to the (formally) intractable problem of exact ground-state preparation. However, as faithful imaginary time evolution produces an exponentially decaying infidelity with the final state, the long-time algorithm may not be needed if sufficient fidelity is already reached. For finite imaginary time, as needed in thermal state simulation or to prepare the more general class of states discussed above, the concerns are also less relevant. In addition, various heuristics may be used to ameliorate these above concerns. We now turn to the discussion of heuristics, before studying the potential issues at finite and at long imaginary times through numerical simulations.

B. Locality heuristic

To address the growing nonlocality of $\tilde{H}$ we first write a modified generating equation for $\tilde{H}$, with separate differential equations for the individual terms $\tilde{h}_\beta$. We choose $|\Psi(0)\rangle$ such that it is annihilated by each $\tilde{h}_\beta(0)$ and the evolution preserves this annihilation condition, analogous to Eq. (4). We consider

$$\frac{d\tilde{h}_\beta}{d\tau} = \sum_\alpha \{\tilde{h}_\beta, h_\alpha\}', \quad (6)$$

where $\{a, b\}'$ denotes the anticommutator of a and b if they do not commute and zero if they do. Equation (6) also satisfies the adiabatic trajectory of Eq. (3) because (4) and (6) only differ by terms that annihilate $|\Psi(\tau)\rangle$; so far no heuristic has been introduced. The expression $\{\tilde{h}_\beta, h_\alpha\}'$ means that $\tilde{H}$ no longer contains geometrically nonlocal terms: each $\tilde{h}_\beta$ grows its support from the contribution of terms h_α that overlap with the boundary of its support at every step.

We can then introduce a heuristic to control the width of support. In particular, we can truncate summation over α in Eq. (6) so that only a subset of terms h_α are retained for each $\tilde{h}_\beta$. More precisely, a neighborhood block is assigned to every $\tilde{h}_\beta$ term which is a region with a given spatial extent w that surrounds the location of $\tilde{h}_\beta$ at $\tau = 0$; every h_α term that lies in the neighborhood block of $\tilde{h}_\beta$ is retained in Eq. (6). In this approximation, $\tilde{H}$ remains strictly w-geometrically local with time. We note that this above heuristic is different from the locality approximation in the original QITE algorithm, as it is a direct restriction on the operator, rather than the correlation length of the imaginary-time-evolved state. The relationship between the two is studied numerically below.

C. Gauge degree of freedom

We can introduce other modifications to the generating equation of $\tilde{H}$ which do not modify the imaginary time evolution trajectory but which can, in principle, affect $||\tilde{H}||$ and its spectrum. Consider, for example,

$$\frac{d\tilde{h}_\beta}{d\tau} = \sum_\alpha \{\tilde{h}_\beta, h_\alpha\}' + f(\tilde{h}_\beta), \quad (7)$$

where $f(\tilde{h}_\beta(\tau))$ annihilates $\Psi(\tau)$. This ensures that the ground state of $\tilde{H}$ is a zero eigenstate for all τ (although it does not ensure that it is always the ground state). We can then optimize $f(\tilde{h}_\beta)$ to control the gap and norm. Specifically, in tests below, we consider $f(\tilde{h}_\beta) = u_1\tilde{h}_\beta - u_2\tilde{h}_\beta^2$. The u_1 term is equivalent to adding a constant shift to H in Eq. (4). While we do not expect this gauge choice to remove the fundamental difficulties of preparing states for infinite imaginary times, we can expect to improve the preparation of states for finite imaginary time. In practice, we do not know how to choose $f(u)$ ahead of time, but it may be chosen in a heuristic manner or $f(u)$ may be chosen as part of a variational ansatz for $\Psi(\tau)$ at finite τ.

III. NUMERICAL SIMULATIONS

We now study the imaginary time trajectory generated by the $\tilde{H}$ dynamics, including the locality and gauge modifications described above. We classically propagate $\tilde{H}$ by a second-order Runge-Kutta method [23] with a finite time step ϵ [error $O(\epsilon^3)$ per time step; note we use ϵ rather than $d\tau$ here to emphasize a finite step] and then diagonalize $\tilde{H}(\tau)$ to study the trajectory of the ground state $\Phi_0(\tau)$. We then monitor various quantities, such as $||\tilde{H}(\tau)||$, the gap $\tilde{\Delta}(\tau)$, the infidelity with the exact imaginary time propagated state $I^\tau(\tau) = 1 - |\langle\tilde{\phi}_0(\tau)|\Psi(\tau)\rangle|^2$, and the infidelity with the ground state of H, $I^\infty(\tau) = 1 - |\langle\tilde{\phi}_0(\tau)|\Psi(\infty)\rangle|^2$, i.e., the outcome of the infinite imaginary time evolution.
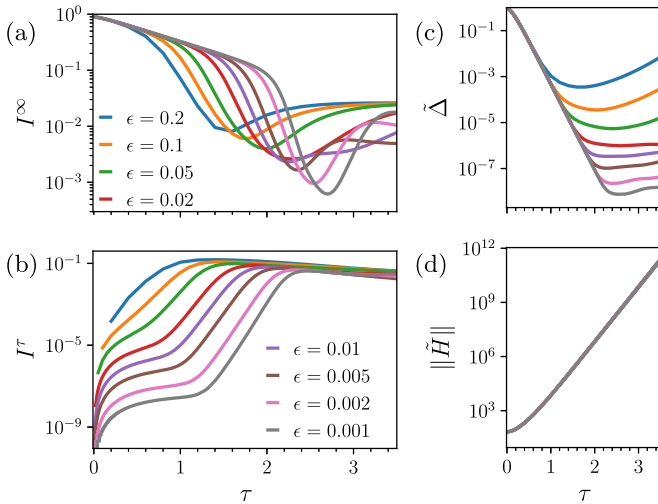
FIG. 1. Adiabatic evolution under the Hamiltonian $\tilde{H}$ for a Heisenberg XXZ system of length $L = 8$. $\tilde{H}$ is generated by integrating Eq. (4) with second-order Runge-Kutta and time-step ϵ, which is varied here. I^∞, I^τ: infidelities with the ground state of H and with the exact imaginary time evolved state; $\tilde{\Delta}$: instantaneous gap of $\tilde{H}$; $||\tilde{H}||$: norm of $\tilde{H}$. The same color is used in all of the plots for each value of ϵ, even though we have shown each ϵ only once.

We study the antiferromagnetic Heisenberg XXZ model in one dimension with open boundary conditions:

$$H_{\lambda_z} = \sum_j S_j^x S_{j+1}^x + S_j^y S_{j+1}^y + \lambda_z S_j^z S_{j+1}^z, \quad (8)$$

with $\lambda_z = 2$, which results in an Ising-like anisotropy. To generate a simple initial state, we initialize the adiabatic Hamiltonian $\tilde{H}$ as a staggered transverse field: $\tilde{H}(\tau = 0) = \sum_j [(-1)^j S_j^x + \frac{1}{2}]$ (where each term in brackets separately annihilates the ground state); the resulting initial state is thus a product state. We then determine $\tilde{H}$ under the dynamics generated by Eqs. (4), (6), and (7), and study various properties of $\tilde{H}$ and its instantaneous ground state $\tilde{\phi}_0(\tau)$, which is intended to produce the imaginary-time trajectory. $\tilde{H}$ has the symmetry $\prod_i S_i^x$, under which $\tilde{\phi}_0(\tau)$ has a definite eigenvalue. Note that $H_{\lambda_z=2}$ has symmetry broken ground states with long range order [24,25], but we take $|\Psi(\infty)\rangle$ to belong to the same symmetry sector as $\tilde{\phi}_0(\tau)$.

In Fig. 1 we first consider $\tilde{H}$ generated by Eq. (4) and the infidelities $I(\tau)$, $I^\infty(\tau)$, $||\tilde{H}(\tau)||$, and $\tilde{\Delta}(\tau)$ as a function of time-step ϵ used in the classical integration of Eq. (4). As seen, for all step sizes, at early times the infidelity with the ground state of H, $I^\infty(\tau)$, decreases exponentially quickly, to 10^{-2} or less. [Although this is a small system, we note that achieving finite infidelities of $O(10^{-1})$ is already important for ground-state preparation applications as it enables variants of quantum phase estimation adapted to the near-term setting [26]]. The achieved infidelities decrease as ϵ is decreased towards an infinitesimal step size in the classical integrator, which would give $I^\tau(\tau) = 0$ at all times and $I^\infty(\tau) \to 0$ at long times. For a finite step size ϵ, we see $I^\infty(\tau)$ reaches a minimum value, while $I^\tau(\tau)$ first increases with time, reaches a maximum, and then plateaus. The time for the minimum I^∞ is close to (slightly after) the time for the maximum I^τ;
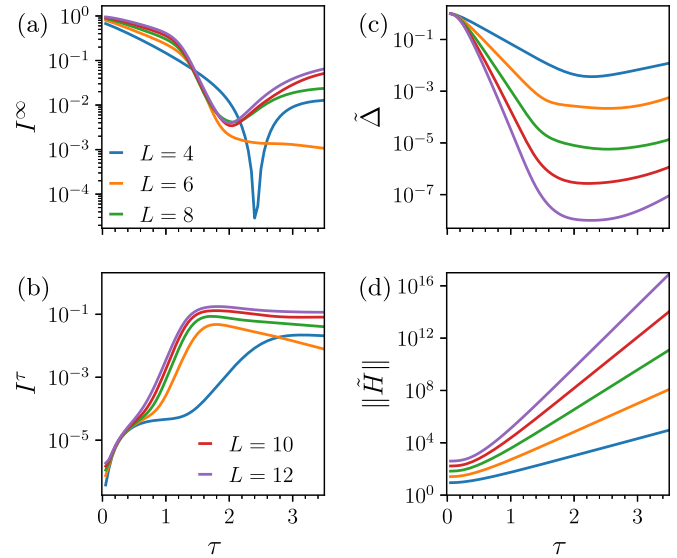

FIG. 2. Adiabatic evolution under $\tilde{H}$ generated by Eq. (6), for the Heisenberg XXZ system as a function of chain length L. $\tilde{H}$ is generated using second-order Runge-Kutta and a time step of $\epsilon = 0.05$. Quantities are the same as in Fig. 1.

we refer to this (approximate) time as τ_c. $||\tilde{H}||$ increases exponentially, while $\tilde{\Delta}$ decreases exponentially until about τ_c, before slowly increasing again. The above is consistent with our analysis that for a finite time step it is only possible to determine the adiabatic Hamiltonian accurately up to a maximum time τ_c.

We next study $\tilde{H}$ generated by the exact Eq. (6), i.e., without enforcing locality, as a function of system size L and a fixed classical time step $\epsilon = 0.05$ in Fig. 2. The results are similar to those using $\tilde{H}$; both formally generate the exact imaginary-time trajectory for infinitesimal step size. Using a finite time step, examining I^∞, I^τ, we see the same behavior of reaching a minimum I^∞ and a maximum I^τ at some approximate time τ_c. Surprisingly, this does not seem to change the maximum reliable propagation time, $\tau_c \approx 1.8$, between $L = 6$ and 12.

The above two numerical studies illustrate the formal exactness of the A-QITE procedure, as well as the numerical challenges in its implementation arising from the behavior of $||\tilde{H}(\tau)||$ and $\tilde{\Delta}(\tau)$. We now study the impact of heuristics at controlling these quantities. We first apply the locality heuristic for the generation of $\tilde{H}$, implemented using Eq. (6) with finite width $w = 5$ in Fig. 3. We study a range of system sizes and integration time steps. Although the finite width means that we no longer follow the imaginary-time trajectory exactly (even for infinitesimal time step), we still see exponential decay of the infidelity with the ground state to useful values of $\sim 10^{-2}$ or less. Overall, the infidelity dynamics shows similar behavior to previous examples and at longer times there is a τ_c corresponding to a change in the behavior of the infidelities and gaps. However, as the time step goes to 0, the minimum I_∞ does not keep decreasing, because of the finite width error. From the perspective of the classical integration and quantum implementation, the dynamics generated under the locality heuristic is much more favorable than under the exact A-QITE $\tilde{H}$ dynamics. In particular, $||\tilde{H}||$ grows orders of magnitude
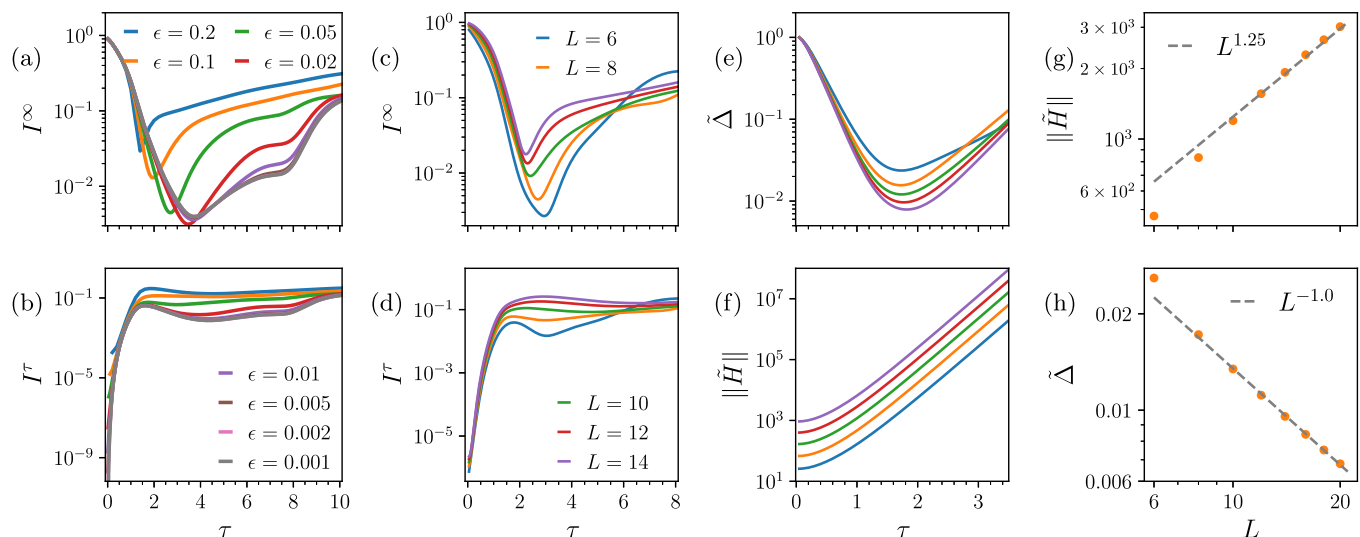
FIG. 3. Adiabatic evolution under $\tilde{H}$ generated by Eq. (6), using a locality truncation with block size $w = 5$, for Heisenberg XXZ chains of various lengths. Panels (a) and (b) show infidelities for different values of ϵ and $L = 8$. Note that the infidelities are defined in the same way as in Fig. 1. Panels (c) and (d) show the behavior of the infidelities for different lengths, second-order Runge-Kutta, $\epsilon = 0.05$. Panels (e) and (f) depict the gap and norm for different lengths; the same colors as the second column are used. Panels (g) and (h) denote the norm and the gap of the adiabatic Hamiltonian as a function of length. The data is consistent with power-law behaviors for both.

more slowly with τ and (for fixed τ) close to linearly with L, while $\tilde{\Delta}$ appears to decrease like poly$(1/L)$.

In Fig. 4, we show $\tilde{H}$ generated by Eq. (6), using the locality heuristic with widths 3, 5, 7, and time step $\epsilon = 0.05$, as well as a protocol where the width is increased at increasing times. For comparison, we also show data from the original quantum imaginary time evolution scheme with widths 2, 4, 6 and for time step $\epsilon = 0.08$. As expected, the best achievable fidelity with the exact state $I^\infty(\tau)$ increases with w; however, the best $I(\infty)$ in fact decreases moving from $w = 5$ to $w = 7$. Compared to the original QITE scheme, the achievable infidelity appears to be better (i.e., lower) using the adiabatic
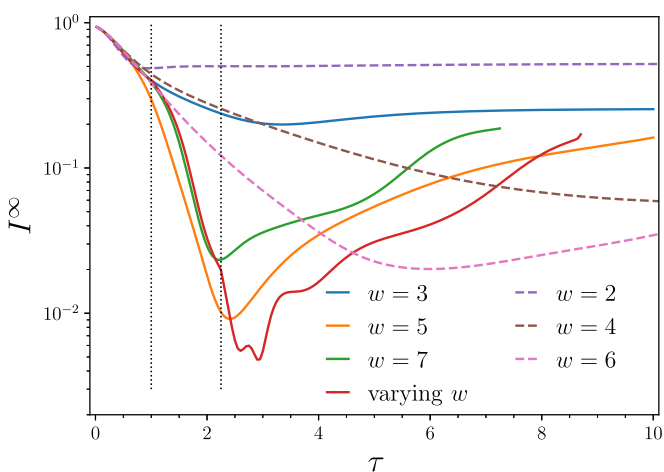

FIG. 4. Infidelity with the desired ground state for both the adiabatic QITE and the original QITE algorithm. Even values of w correspond to the original QITE algorithm and the odd w values and the varying case corresponds to the adiabatic QITE. The time steps are taken as 0.05 for A-QITE and 0.08 for QITE. The varying w case starts with $w = 3$, then changes to $w = 5$, and ultimately to $w = 7$. The positions of the transitions are shown by vertical dotted lines.

Hamiltonian $\tilde{H}$ with a similar locality definition. Further work is required to establish a more precise relationship between these approximations.

We additionally consider the modified $\tilde{H}$ generated in a different gauge using Eq. (7). As an illustrative example, we consider the case $u_1 = 1/2$, $u_2 = 2$, with the locality constraint $w = 5$. In Fig. 5, we see that, although the behavior of the infidelities I_∞ and I^τ are qualitatively similar to what we have seen previously (corresponding to $u_1 = u_2 = 0$) with a similar τ_c, the detailed form is different; for example, the infidelity has a flatter plateau region. In addition, $||H||$ grows even more slowly with τ (with a flattened region between $\sim 1 < \tau < 3$) while still being close to linear in L, while Δ (at τ_c) again appears to have a poly$(1/L)$ behavior. This indicates that a suitable choice of $f(u)$ can meaningfully modify the dynamics and the achievable infidelities at finite times.

We now briefly discuss the implications for implementations in the near-term setting. For a given width w and Trotter time step, the gate cost of implementing an A-QITE time step is the same as that of QITE, namely it is the cost to implement a time step under a w-qubit unitary and importantly the A-QITE time step requires no measurements. However, one difference with the original QITE is the need to maintain adiabaticity during the A-QITE simulation, which governs the time of Hamiltonian simulation for the given τ. The (limited) numerical data above on the scaling of $\tilde{H}$ and $\tilde{\Delta}$ when using the heuristic modifications in the Ising problem suggest that (for given τ) the total adiabatic evolution time is polynomial in system size [as $||H||, ||\tilde{H}||$ scale like poly(L) and $\tilde{\Delta} \sim$ poly$(1/L)$]. The Hamiltonian simulation is still likely the most challenging aspect of the algorithm for near-term hardware. However, for modest widths, e.g., $w = 3$, implementing the A-QITE protocol is similar to implementing ASP with geometric three-local Hamiltonians, which has already been demonstrated on near-term hardware using error mitigation and circuit recompilation [27]. Alternatively, it may be
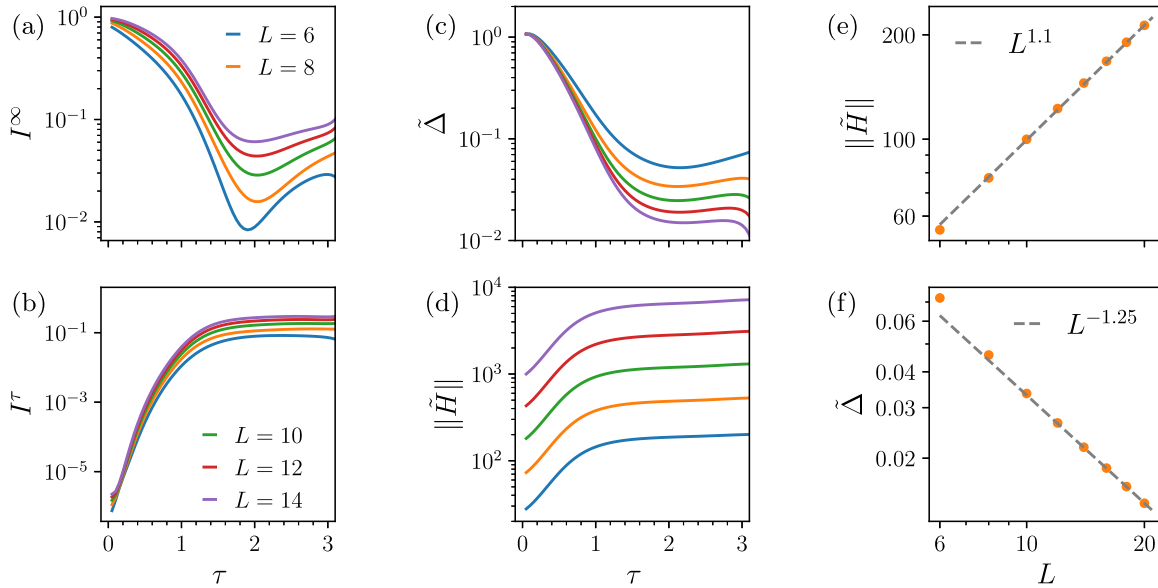
FIG. 5. Adiabatic evolution under $\tilde{H}$ generated by Eq. (7) with $u_1 = 2$, $u_2 = 0.5$, block size $w = 5$, second-order Runge-Kutta, $\epsilon = 0.05$, for the Heisenberg XXZ system for various lengths. Quantities same as in Fig. 1. Panels (e) and (f) denote the norm and the gap of the adiabatic Hamiltonian as a function of length. The data is consistent with power-law behaviors for both.

beneficial to relax the adiabaticity requirement by employing A-QITE within a version of the quantum approximation optimization algorithm (QAOA) [4,28], where $\tilde{H}$ provides the form of the operators in the ansatz.

IV. CONCLUSIONS

We have described an adiabatic state preparation protocol that implements the imaginary time evolution trajectory without any need for quantum tomography or ancilla resources. This hybrid algorithm involves a classical time integration to generate the adiabatic Hamiltonian, but does not require any measurements on the quantum system. When implemented faithfully, the algorithm leads to an exponential decrease of the infidelity with the ground state of a desired Hamiltonian with adiabatic time. However, the cost of evolving exactly to long imaginary times grows rapidly with imaginary time both in the classical and quantum parts of the protocol. The growth in cost as a function of imaginary time arises from several sources, including the nonlocality of the derived adiabatic Hamiltonian. We introduce a heuristic to control this nonlocality by truncating terms in the adiabatic Hamiltonian. Another source of growing cost at long imaginary time is related to the norm of the adiabatic Hamiltonian and its gap. We show that modifying the generating equation of the adiabatic Hamiltonian can be used to control these quantities at finite imaginary times. Both heuristics enable one to propagate for short times

and to observe a large improvement in the approximate ground state.

In the near-term quantum hardware setting, one advantage of the current approach is that each time step can be implemented without measurements. On the other hand, preserving the strict adiabatic formulation may lead to long Hamiltonian simulation times for some problems.

More generally, the A-QITE procedure we have introduced extends the types of states that be generated using an adiabatic simulation protocol; the target state need not be expressed as the ground state of a known Hamiltonian, but rather can be expressed implicitly through the differential evolution of a known ground state. In addition, with respect to standard ground-state adiabatic state preparation, A-QITE expands the set of possible adiabatic paths. This potentially allows for introduction of new quantum adiabatic routines consisting of composite adiabatic paths (with A-QITE as one of them) with applications such as the introduction of novel adiabatic catalysts [8,29] as directions to be explored in the future.

[1] J. Preskill, Quantum computing in the NISQ era and beyond, Quantum **2**, 79 (2018).

[2] B. Bauer, S. Bravyi, M. Motta, and G. K.-L. Chan, Quantum algorithms for quantum chemistry and quantum materials science, Chem. Rev. **120**, 12685 (2020).

[3] A. Peruzzo, J. McClean, P. Shadbolt, M.-H. Yung, X.-Q. Zhou, P. J. Love, A. Aspuru-Guzik, and J. L. O'brien, A varia-

tional eigenvalue solver on a photonic quantum processor, Nat. Commun. **5**, 4213 (2014).

[4] E. Farhi, J. Goldstone, and S. Gutmann, A quantum approximate optimization algorithm, arXiv:1411.4028.

[5] J. R. McClean, J. Romero, R. Babbush, and A. Aspuru-Guzik, The theory of variational hybrid quantum-classical algorithms, New J. Phys. **18**, 023023 (2016).

[6] C. Schön, K. Hammerer, M. M. Wolf, J. I. Cirac, and E. Solano, Sequential generation of matrix-product states in cavity QED, Phys. Rev. A **75**, 032311 (2007).

[7] J. Romero, R. Babbush, J. R. McClean, C. Hempel, P. J. Love, and A. Aspuru-Guzik, Strategies for quantum computing molecular energies using the unitary coupled cluster ansatz, Quantum Sci. Technol. **4**, 014008 (2018).

[8] T. Albash and D. A. Lidar, Adiabatic quantum computation, Rev. Mod. Phys. **90**, 015002 (2018).

[9] R. Babbush, P. J. Love, and A. Aspuru-Guzik, Adiabatic quantum simulation of quantum chemistry, Sci. Rep. **4**, 6603 (2014).

[10] L. Veis and J. Pittner, Adiabatic state preparation study of methylene, J. Chem. Phys. **140**, 214111 (2014).

[11] S. McArdle, T. Jones, S. Endo, Y. Li, S. C. Benjamin, and X. Yuan, Variational ansatz-based quantum simulation of imaginary time evolution, npj Quantum Inf. **5**, 75 (2019).

[12] M. Motta, C. Sun, A. T. K. Tan, M. J. O'Rourke, E. Ye, A. J. Minnich, F. G. S. L. Brandão, and G. K. Chan, Determining eigenstates and thermal states on a quantum computer using quantum imaginary time evolution, Nat. Phys. **16**, 205 (2020).

[13] S.-N. Sun, M. Motta, R. N. Tazhigulov, A. T. K. Tan, G. K.-L. Chan, and A. J. Minnich, Quantum computation of finite-temperature static and dynamical properties of spin systems using quantum imaginary time evolution, PRX Quantum **2**, 010317 (2021).

[14] K. Yeter-Aydeniz, R. C. Pooser, and G. Siopsis, Practical quantum computation of chemical and nuclear energy levels using quantum imaginary time evolution and Lanczos algorithms, npj Quantum Inf. **6**, 63 (2020).

[15] N. Gomes, F. Zhang, N. F. Berthusen, C.-Z. Wang, K.-M. Ho, P. P. Orth, and Y. Yao, Efficient step-merged quantum imaginary time evolution algorithm for quantum chemistry, J. Chem. Theory Comput. **16**, 6256 (2020).

[16] H. Nishi, T. Kosugi, and Y.-i. Matsushita, Implementation of quantum imaginary-time evolution method on NISQ devices by introducing nonlocal approximation, npj Quantum Inf. **7**, 85 (2021).

[17] H. Kamakari, S.-N. Sun, M. Motta, and A. J. Minnich, Digital quantum simulation of open quantum systems using quantum imaginary–time evolution, PRX Quantum **3**, 010320 (2022).

[18] K. Yeter-Aydeniz, E. Moschandreou, and G. Siopsis, Quantum imaginary-time evolution algorithm for quantum field theories with continuous variables, Phys. Rev. A **105**, 012412 (2022).

[19] E. Farhi, J. Goldstone, S. Gutmann, and M. Sipser, Quantum computation by adiabatic evolution, arXiv:quant-ph/0001106.

[20] A. Messiah, *Quantum Mechanics* (Courier Corporation, North Chelmsford, MA, 2014).

[21] T. Kosugi, Y. Nishiya, H. Nishi, and Yu-ichiro Matsushita, Imaginary-time evolution using forward and backward real-time evolution with a single ancilla: First-quantized eigensolver algorithm for quantum chemistry, Phys. Rev. Res. **4**, 033121 (2022).

[22] A. M. Childs, Y. Su, M. C. Tran, N. Wiebe, and S. Zhu, Theory of trotter error with commutator scaling, Phys. Rev. X **11**, 011020 (2021).

[23] In the same fashion as Ref. [12], we take the effect of separate terms of H into account separately for $\tilde{H}$, so each time step consists of a sequence of substeps, each one propagating for time ϵ with a single term of H.

[24] R. Orbach, Linear antiferromagnetic chain with anisotropic coupling, Phys. Rev. **112**, 309 (1958).

[25] H.-J. Mikeska and A. K. Kolezhuk, One-dimensional magnetism, *Quantum Magnetism*, Lecture Notes in Physics Vol 645 (Springer, Berlin, Heidelberg, 2004), pp. 1–83.

[26] Z. Ding and L. Lin, Even shorter quantum circuit for phase estimation on early fault-tolerant quantum computers with applications to ground-state energy estimation, PRX Quantum **4**, 020331 (2023).

[27] A. T. K. Tan, S.-N. Sun, R. N. Tazhigulov, G. K.-L. Chan, and A. J. Minnich, Realizing symmetry-protected topological phases in a spin-1/2 chain with next-nearest-neighbor hopping on superconducting qubits, Phys. Rev. A **107**, 032614 (2023).

[28] K. Blekos, D. Brand, A. Ceschini, C.-H. Chou, R.-H. Li, K. Pandya, and A. Summer, A review on quantum approximate optimization algorithm and its variants, Phys. Rep. **1068**, 1 (2024).

[29] E. Farhi, J. Goldstone, and S. Gutmann, Quantum adiabatic evolution algorithms with different paths, arXiv:quant-ph/0208135.